Pis'ma v ZhETF, vol. 98, iss. 3, pp. 183 – 186

Thermodynamics of electron-hole liquids in graphene

L. A. Falkovsky

Landau Institute for Theoretical Physics of the RAS, 119334 Moscow, Russia

Verechagin Institute of the High Pressure Physics of the RAS, 142190 Troitsk, Russia

Submitted 24 June 2013

The impact of Coulomb interactions on the chemical potential, heat capacity, and oscillating magnetic moment is studied. The cases of low and high temperatures are considered. At low temperatures, doped graphene behaves as the common Fermi liquids with the power temperature laws for thermodynamic properties. However, at high temperatures and relatively low carrier concentrations, it exhibits the collective electron- holes behavior: the chemical potential tends to its value in the undoped case going with the temperature to the charge neutrality point. Simultaneously, the electron contribution into the heat capacity tends to the constant value as in the case of the Boltzmann statistics.

DOI: 10.7868/S0370274X13150083

I. Introduction. Optic and magneto-optic experiments with graphene layers have been successfully interpreted [1] so far in a scheme of massless relativistic particles with a conical energy spectrum

$$\varepsilon_s(p) = \mp vp, \tag{1}$$

where v is the constant velocity parameter for two bands, $s = 1, 2$, in the neighborhood of the K-points in the Brillouin zone. In pure graphene, the chemical potential is situated at the charge neutrality point $\varepsilon = 0$. However, the chemical potential can possesses a nonzero value because of doping or under a gate voltage. Thus, the chemical potential is determined by the total number of carriers (difference of electrons in the upper band and holes in the low band)

$$N = 4S \int |f(\varepsilon - \mu) - f(\varepsilon + \mu)| \frac{d^2\mathbf{p}}{(2\pi\hbar)^2}, \tag{2}$$

where $f(\varepsilon - \mu)$ is the Fermi function, S is the surface of the graphene layer, and the factor 4 takes the valley and spin degeneracy into account. The integration is performed over $\varepsilon > 0$, the chemical potential is positive for electrons and negative for holes. At the fixed N, this condition determines the dependence $\mu(T)$, shown in Fig. 1 for a relatively low electron concentration.

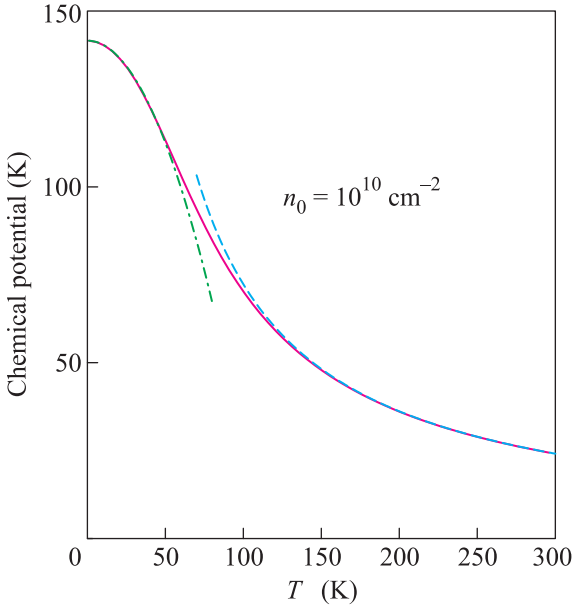

Fig. 1. Chemical potential versus temperature for the carrier concentration $10^{10}\,\mathrm{cm}^{-2}$; the Coulomb renormalization is not included. The exact solution to Eq. (2) is indicated by the solid line, the dashed-dotted lines show the asymptotes for low and high temperatures (see text)

For the conical spectrum, Eq. (1), the ratio between the kinetic and Coulomb energies has a constant value independently of the carrier concentration and the problem of the phase electron-dielectric transition appears. It was recently discovered [2] in studying of the Shubnikov-de Haas oscillations that electron-electron interactions are very important for low carrier concentrations. While the electron concentration decreases from 10^{12} to $10^9\,\mathrm{cm}^{-2}$, the velocity parameter v grows by three times from its ordinary value $1.05 \cdot 10^8$ cm/s. The logarithmic renormalization of the velocity for the linear electron dispersion was found by Abrikosov and Beneslavsky [3] in the three-dimensional case and in Refs. [4–7] for two-dimensional graphene. Notice, that no phase transition was revealed even at the lowest carrier concentration. We can conclude that

screening Coulomb interactions do not create any gap in the spectrum.

The renormalized electron dispersion can be written in the form

$$\varepsilon_s(p) = \mp vp[1 + g\ln(p_0/p)], \tag{3}$$

where $g = e^2/8\pi\hbar v\epsilon$ is the dimensionless electron-electron interaction and $\epsilon \simeq 2.5{-}8$ describes an effect of a substrate and self-screening in graphene, the cutoff parameter $p_0 \simeq 0.5 \cdot 10^8\,\mathrm{cm}^{-1}$ is estimated in Refs. [2].

Equation (3) is written in the linear approximation in $g\ln(p_0/p) < 1$. Because the logarithm is assumed to be large, the condition $g \ll 1$ has to be fulfilled, and we suppose this condition in what followed. Using Eqs. (2), (3), we evaluate the screening effect on the chemical potential demonstrated in Fig. 2 at the carrier concentration $n_0 = 10^{11}\,\mathrm{cm}^{-2}$. Results for limiting cases of low and high temperatures are obtained below in the analytical form. In this paper, we consider the impact of renormalization on the thermodynamic properties of graphene such as the chemical potential, heat capacity, and magnetic moment.

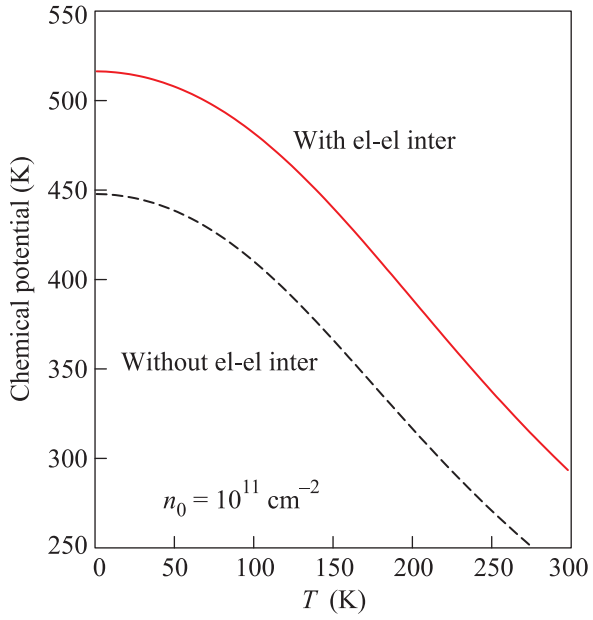

Fig. 2. Chemical potential as a function of temperature for the carrier concentration $10^{11}\,\mathrm{cm}^{-2}$; the renormalization is included (solid line), the chempotential for noninteracting electrons is shown in the dashed line; the cutoff parameter $p_0 = 0.5 \cdot 10^8\,\mathrm{cm}^{-1}$, the dielectric constant $\epsilon = 2.5$; the interaction constant $g = 0.0367$

II. Temperature dependence of the chemical potential. For low ($\mu \gg T$) and high ($\mu \ll T$) temperatures, the analytical expressions for $\mu(T)$ can be obtained from Eq. (2) with the renormalization taken into account.

For low temperatures, it is convenient to differentiate Eq. (2) with respect the temperature, using

$$\frac{df\left[\varepsilon - \mu\left(T\right)\right]}{dT} = \left(\frac{\varepsilon - \mu}{T} + \frac{d\mu}{dT}\right)\left[-\frac{\partial f\left(\varepsilon - \mu\right)}{\partial \epsilon}\right].$$

Here, we have a sharp function of $(\varepsilon - \mu)$. Therefore, in the integrand, the momentum

$$p = \varepsilon[1 - g\ln(p_0 v/\varepsilon)]/v$$

should be expand near $\varepsilon = \mu$ in powers of $(\varepsilon - \mu)$, which gives a factor proportional to T after the integration. For instance, we get in the case of electron doping

$$0 = \int_{-\infty}^{\infty}\left[-\frac{\partial f\left(\varepsilon - \mu\right)}{\partial \epsilon}\right]\left[\mu\frac{d\mu}{dT} + \frac{(\varepsilon - \mu)^2}{T}\right] \times \\ \times\,[1 - 2g\ln(p_0 v/\mu)]d\varepsilon,$$

where we do not differentiate the logarithm because of the condition $g \ll 1$. Integrating, one finds

$$\frac{d\mu}{dT} = -\frac{\pi^2}{3\varepsilon_\mathrm{F}}T, \tag{4}$$

where we denote $\varepsilon_\mathrm{F} \equiv \mu(T = 0)$, positive for electrons and negative for holes. Let us notice that this is the known temperature dependence of the chemical potential in the degenerate Fermi system at low temperatures. We emphasize that the Fermi energy ε_F is determined indeed by the carrier concentration

$$n_0 = \frac{p_\mathrm{F}^2}{\pi\hbar^2} = \frac{1}{\pi}\left(\frac{\varepsilon_\mathrm{F}}{\hbar v}\right)^2[1 - 2g\ln(p_0 v/|\varepsilon_\mathrm{F}|)], \tag{5}$$

which introduces the renormalization in Eq. (4) by means of ε_F.

For high temperatures, we can expand the integrand of Eq. (2) in μ. Introducing the new variable $x = \varepsilon/2T$, we get the integral

$$N = \frac{4|\mu|ST}{\pi(\hbar v)^2}\int_0^\infty \frac{1 - 2g\ln(p_0 v/2Tx)}{\cosh^2 x}x dx\,,$$

which gives the chemical potential

$$|\mu| = \frac{\pi}{4\ln 2}\frac{n_0(\hbar v)^2}{T}[1 + 2g\ln(p_0 v/2T)]\,. \tag{6}$$

We see the inverse temperature dependence of the chemical potential, as a collective effect in electron-hole liquids. The renormalization term, correcting the temperature dependence, is presented here explicitly and illustrated in Fig. 3.

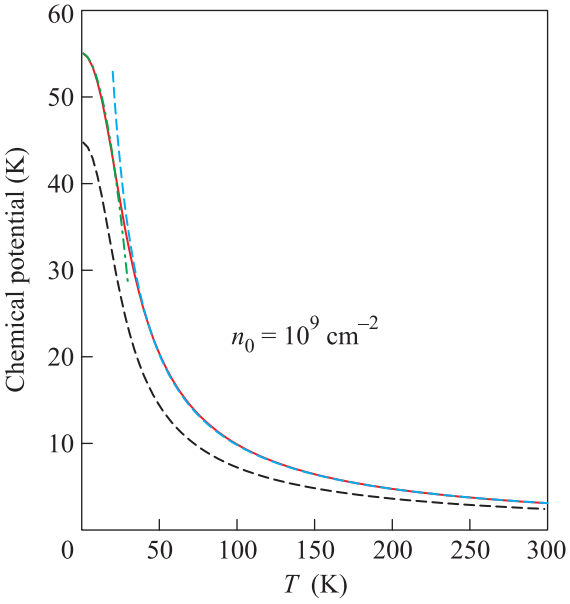

Fig. 3. Chemical potential versus temperature for the carrier concentration $10^9\,\mathrm{cm}^{-2}$; the renormalization is included (solid line), the dashed-dotted lines are asymptotes for low and high temperatures, the chempotential for non-interacting electrons is shown in the dashed lines; other parameters are the same as in Fig. 2

III. Heat capacity. Now we consider the electron contribution to the heat capacity. The energy of carriers

$$E = 4S\int_0^\infty \varepsilon |f(\varepsilon-\mu) - f(\varepsilon+\mu)|\frac{d^2\mathbf{p}}{(2\pi\hbar)^2} \qquad (7)$$

differs from the carrier concentrations, Eq. (2), only by the additional factor ε in the integrand. Therefore, we can follow the same procedure.

For low temperatures, $T \ll \varepsilon_\mathrm{F}$, the carrier heat capacity in the case of electron doping writes as

$$C_S^{(e)} = \frac{2S}{\pi(\hbar v)^2}\int_{-\infty}^{\infty}\left[\mu^2\frac{d\mu}{dT} + 2\mu\frac{(\varepsilon-\mu)^2}{T}\right]\times$$
$$\times\left[-\frac{\partial f(\varepsilon-\mu)}{\partial\varepsilon}\right][1-2g\ln(p_0v/\mu)]d\varepsilon =$$
$$= \frac{2S}{\pi(\hbar v)^2}\left[\mu^2\frac{d\mu}{dT} + \frac{2\pi^2}{3}\mu T\right][1-2g\ln(p_0v/\mu)].$$

Using Eq. (4), we have

$$C_S^{(e)} = \frac{2\pi S|\varepsilon_\mathrm{F}|}{3(\hbar v)^2}T[1-2g\ln(p_0v/|\varepsilon_\mathrm{F}|)]$$

in both cases of the electron or hole carriers.

For high temperatures, $T \gg \mu$, one can perform the expansion of the energy, Eq. (7), in the first order of μ

$$E = \frac{4S|\mu|}{\pi(\hbar v)^2}\int_0^\infty \varepsilon^2\left[-\frac{\partial f(\varepsilon)}{\partial\varepsilon}\right][1-2g\ln(p_0v/\varepsilon)]d\varepsilon =$$
$$= \frac{2\pi S|\mu|}{3(\hbar v)^2}T^2[1-2g\ln(p_0v/2T)].$$

Using Eq. (6), we find

$$E = \frac{\pi^2}{6\ln 2}NT \quad\text{and}\quad C_S^{(e)} = \frac{\pi^2}{6\ln 2}N.$$

Finally,

$$C_S^{(e)} = \frac{\pi^2}{3}N\begin{cases} 2\dfrac{T}{|\varepsilon_\mathrm{F}|}, & T \ll |\mu|, \\ \dfrac{1}{2\ln 2}, & T \gg |\mu|. \end{cases} \qquad (8)$$

Thus, we see that the renormalization modifies the heat capacity at low temperatures, i.e., in the degenerate statistics. At high temperatures, the heat capacity possesses the constant value and does not reveal any renormalization at least to a first approximation in $g\ln(p_0/p)$.

IV. Magnetic susceptibility. Magnetic susceptibility is determined by the dependence of the thermodynamic potential on the magnetic field

$$\Omega(B) = -\frac{2eBTS}{\pi\hbar c}\sum_{n,s}\ln\left(1+e^{\frac{\mu-\varepsilon_{sn}}{T}}\right)$$

in terms of the electron dispersion ε_{sn} for two bands $s = 1, 2$ with the Landau number $n = 0, 1, 2, \ldots$ We neglect the spin splitting of the levels in comparison with the large Landau splitting in graphene.

Oscillations of the magnetic moment in the semi-classical region can be found applying the Poison formula to the thermodynamic potential

$$\Omega(B) = -\frac{2eBTS}{\pi\hbar c}\sum_{k\neq 0}\int_0^\infty\left[\ln\left(1+e^{\frac{\mu-\varepsilon}{T}}\right) + \right.$$
$$\left. + \ln\left(1+e^{\frac{\mu+\varepsilon}{T}}\right)\right]e^{2\pi ikn}dn,$$

where the contributions of two bands are written explicitly. The integration by parts gives

$$\Omega(B) = -\frac{eBTS}{\pi^2\hbar c}\sum_{k\neq 0}\int_0^\infty\frac{1}{ik}[f(\varepsilon-\mu)-f(-\varepsilon-\mu)]e^{2\pi ikn}d\varepsilon. \qquad (9)$$

For the semi-classical region, we use the quantization rule in the Bohr–Zommerfeld form

$$2\pi n = \frac{cA(\varepsilon)}{e\hbar B},$$

where the aria enclosed by the electron trajectory for the energy ε in the momentum space writes

$$[A(\varepsilon) = \pi \left(\frac{\varepsilon}{v}\right)^2 [1 - 2g \ln(p_0 v/\varepsilon)]$$

according to Eq. (3).

The main contribution to the integral (9) comes from the vicinity of the point $\varepsilon = \pm\mu(T = 0) = \pm\varepsilon_{\rm F}$ for the positive and negative $\varepsilon_{\rm F}$, correspondingly. Expanding the exponent in the integrand near that points and integrating, one finds

$$\Omega(B) = \frac{2eBTS}{\pi\hbar c} \sum_{k\neq 0} \frac{1}{k} \frac{\sin[kcA(\varepsilon_{\rm F})/e\hbar B]}{\sinh[2\pi^2 kc|m(\varepsilon_F)|T/e\hbar B]},$$

where $m(\varepsilon) = \frac{1}{2\pi}\frac{dA(\varepsilon)}{d\varepsilon}$ is the cyclotron mass. Calculating of the magnetic moment we can derivative only the rapid factor in the argument of sin with respect B:

$$\tilde{M}(B) = \frac{2\pi n_0 ST}{B} \sum_{k\neq 0} \frac{\cos[kcA(\varepsilon_{\rm F})/e\hbar B]}{\sinh[2\pi^2 kc|m(\varepsilon_{\rm F})|T/e\hbar B]}, \quad (10)$$

where the carrier concentration $n_0 = A(\varepsilon_{\rm F})/(\pi\hbar)^2$. This is the standard Lifshiz–Kosevich formula used in Ref. [2] for the interpretation of experimental data concerning the velocity renormalization. There are two important features: first, the aria $A(\varepsilon_{\rm F})$ and the effective mass $m(\varepsilon_{\rm F})$ should be taken at the renormalized Fermi energy corresponding to the carrier concentration and, second, the factor in front of the sum differs from the $3d$-case since the integration over p_z is absent now.

It is interesting to compare the amplitude of oscillations with the monotonic part of the magnetic moment, Refs. [8–10],

$$M_0 = \frac{-S}{6\pi} \left(\frac{ev}{c}\right)^2 \frac{B}{T\cosh^2(\mu/2T)}.$$

Thus, we see that the ratio of the oscillating and monotonic parts of the magnetic moment has the order

$$|\tilde{M}/M_0| \sim 12\pi n_0 \left(\frac{cT}{evB}\right)^2 \frac{\cosh^2(\varepsilon_{\rm F}/2T)}{\sinh[2\pi^2 c|m(\varepsilon_{\rm F})|T/e\hbar B]}.$$

To observe the oscillations, the argument of sinh has to be small or at least on the order of unity. Then, the monotonic part of the magnetic moment can be observable only at relatively high temperatures, $|M_0/\tilde{M}| \sim \sim \exp(-\varepsilon_{\rm F}/T)$.

V. Conclusions. The main issue of the paper is that graphene takes up the intermediate position between metals and semiconductors depending on the carrier concentration. By including the electron spectrum renormalization we have demonstrated that the Coulomb interaction produces the noticeable effects in thermodynamic properties of graphene especially for low carrier concentrations $n_0 < 10^{10}\,{\rm cm}^{-2}$.

At high temperatures, the chemical potential tends to its value in the undoped case going to the charge neutrality point with the temperature. Simultaneously, the carrier contribution to the heat capacity tends to the constant value similar to the case of the Boltzmann statistics.

On the other hand, the chemical potential variation at relatively low temperatures is proportional to the temperature squared with the linear temperature dependence for the heat capacity as in the conventional Fermi liquids.

The effect of the Coulomb renormalization on the magnetic oscillations can be included in the Lifshiz–Kosevich formula involving in the proper way the renormalized effective mass and the aria enclosed by the electron trajectory. However, the pre-exponential factor should be taken as for two-dimension systems.

It should be emphasize two features. First, in comparison to the thermodynamic properties, the optical properties such as the electronic dynamic conductivity are not sensitive to the electron-electron interaction since the conductivity does not depend indeed on the velocity parameter v in the dispersion low of graphene. Second, if the electron interaction is neglected at the thermodynamic studies, the observable data are fitted with the arbitrary increased velocity parameter.

We gratefully acknowledge Andrey Varlamov for useful discussions. This work was supported by the Russian Foundation for Basic Research (grant # 13-02-00244A) and the SIMTECH Program, New Centure of Superconductivity: Ideas, Materials and Technologies (grant # 246937).

1. A. H. Castro Neto, F. Guinea, N. M. R. Peres et al., Rev. Mod. Phys. **8**1, 109 (2009).
2. D. C. Elias, R. V. Gorbachev, A. S. Mayorov et al., Nature Phys. **7**, 701 (2011); G. L. Yu, R. Jalil, B. Belle et al., PNAS **110**(9), 3282 (2013).
3. A. A. Abrikosov and S. D. Beneslavsky, Sov. Phys. JETP **3**2, 699 (1971).
4. J. Gonzalez, F. Guinea, and M. A. H. Vozmediano, Nucl. Phys. B **424**, 595 (1994); Phys. Rev B **59**, 2474 (1999).
5. E. G. Mishchenko, Phys. Rev. Letts. **98**, 216801 (2007).
6. Y. Barlas, T. Pereg-Barnea, M. Polini et al., Phys. Rev. Lett. **98**, 236601 (2007).
7. V. N. Kotov, B. Uchoa, V. M. Pereira et al., Rev. Mod. Phys. **8**4, 1067 (2012).
8. J. W. McClure, Phys. Rev. **104**, 666 (1956).
9. S. A. Safran and F. J. DiSalvo, Phys. Rev. B **20**, 4889 (1979).
10. Y. Ominato and M. Koshino, arXiv:1301.5440.